Nano World Journal

http://dx.doi.org/10.17756/nwj.2015-002

Review Article

Open Access

Determination of Protein-Protein Interaction for Cancer Control via Mass Spectrometry and Nanoconductimetry of NAPPA SNAP Arrays: An Overview

Claudio Nicolini[1,2*], Nicola Luigi Bragazzi[1,2] and Eugenia Pechkova[1,2]

[1]*Nanoworld Institute Fondazione EL.B.A. Nicolini (FEN), Bergamo, Italy*
[2]*Laboratory of Nanobiotechnology and Biophysics (LNB), Department of Experimental Medicine (DIMES), University of Genoa, Genoa, Italy*

***Correspondence to:**
Professor Claudio Nicolini
President, Nanoworld Institute Fondazione EL.B.A. Nicolini (FEN), Largo Redaelli 7, Pradalunga (Bergamo) 24020, Italy
Tel/Fax: +39 035767215
E-mail: president@fondazioneelba-nicolini.org

Received: February 17, 2015
Accepted: March 06, 2015
Published: March 09, 2015

Citation: Nicolini C, Bragazzi NL, Pechkova E. 2015. Determination of Protein-Protein Interaction for Cancer Control via Mass Spectrometry and Nanoconductimetry of NAPPA SNAP Arrays: An Overview. *NanoWorld J* 1(1): 8-16.

Published by United Scientific Group

Abstract

Background: Protein-protein interactions play a major role in Cancer Control and their detailed understanding by Label-Free Nanotechnology is essential especially within the framework of a personalized medicine-based approach.

Material and Methods: We implemented an array of label-free nanobiotechnologies, including the Quartz Crystal Microbalance with Dissipation factor monitoring (QCM_D). We used it for the conductometric monitoring of an antiblastic (temozolomide) interacting with genes and proteins, such as MLH1, that represents a biomarker of the rate survival of patients suffering from brain tumors, outcome of chemotherapy and resistance to drug itself. We coupled the Nucleic Acid Programmable Protein Arrays (NAPPA) and the cell-free protein array with the quartz crystal microbalance technology. In another proof of principle, we coupled the NAPPA with the SNAP tag *E. coli* cell-free expression system. The goal is to analyze the protein-protein interaction using Matrix Assisted Laser Desorption Ionization Time-of-Flight (MALDI-TOF) Bruker Ultraflex and "Protein synthesis Using Recombinant Elements" (PURE) system, thus avoiding the "black box" nature of the cell extract. The *E. coli in vitro* transcription/translation system (IVTT) in respect to the reticulocyte lysate (RRL) or human lysate (HL) is totally characterized and represents an advantage for the subsequent mass spectrometry (MS) analysis. An R Script for Mass Spectrometry Data Preprocessing before Data Mining (SpADS) provides the user with peak recognition and amplitude independent subtraction functions. The MS samples are obtained from SNAP-NAPPA spots and printed on gold coated glass slides in higher density, in order to obtain an amount of protein appropriate for MS analysis.

Conclusion: We developed a coherent approach that overcome the drawbacks and pitfalls of the traditional laborious and time-consuming labeled and fluorescence-based experimental procedures. This, taken together with the unique properties of proteins obtained with Langmuir-Blodgett (LB)-based crystallography that can enable new strategies for drug design separately reported, defines our approach to cancer control.

Keywords

Brain cancer, Cell-free expression system, Conductometer, Nucleic Acid Programmable Protein Array (NAPPA), Quartz Crystal Microbalance with Dissipation factor Monitoring (QCM_D), Temozolomide

Introduction

Together with gene-gene and gene-protein interactions, protein-protein, gene-drug [1-2] and protein-drug [3-4] interactions play a major role in the field of molecular pharmacology as their detailed understanding is essential for improving the mechanisms of the drug itself and to design new chemical compounds, especially within the framework of a personalized medicine-based approach [5-6].

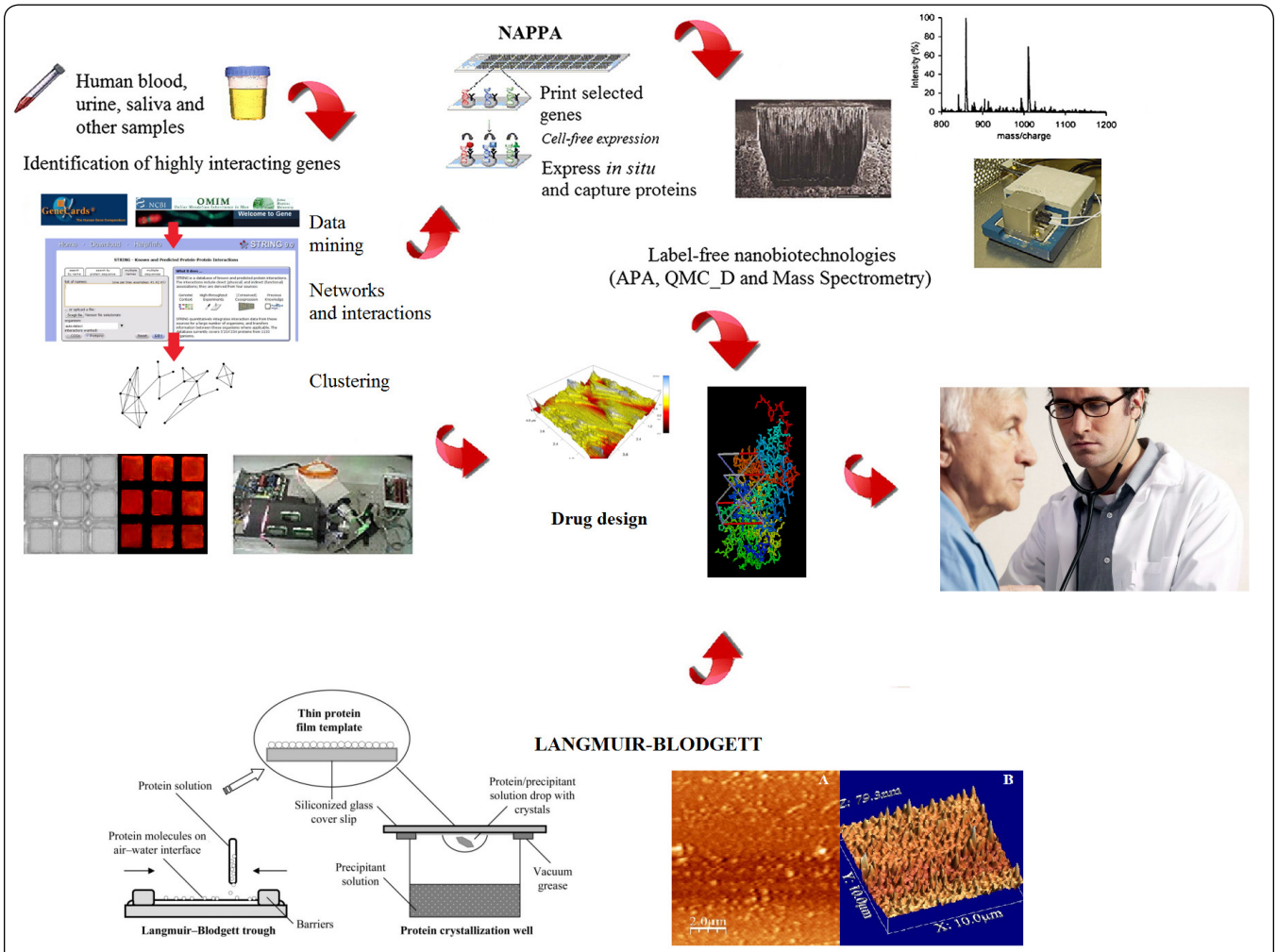

Figure 1: Protocol of the integrated approach for personalized oncology. After collecting the samples from patients (tissue biopsies, blood or other fluids), differentially expressed genes (DEG) are studied using the Leader Gene Algorithm (LGA). Thus, only few genes of interest are selected (genomics signature), which can be used as a panel for monitoring the diseases or can be subsequently expressed via the Nucleic Acid Programmable Protein Array (NAPPA) technology to fully characterize protein–protein interactions (proteomics signature) via label-free nanobiotechnologies (namely, Quartz Crystal Microbalance with Dissipation Factor Monitoring (QCM_D), Anodic Porous Allumina (APA), mass spectrometry (MS)) overcoming the limitations and difficulties encountered in the use of labeled technologies. The unique properties of proteins obtained using the Langmuir-Blodgett (LB)-based crystallography enable optimal drug design.

Our laboratory had previously introduced novel approaches in the field of nanogenomics [7-9] and nanoproteomics [10-11], pioneering in both fields. Only by coupling and combining proteomics and genomics within a highly integrated, coherent framework, with an emphasis on proteomics, clinical problems can be successfully addressed (Figure 1) [12-13].

Mass-scale genomics enables to study the expression of thousands of genes at the same time using high-throughput technologies. However, the analysis and interpretation of the produced data is not a simple task.

The "LeaderGene algorithm" approach [14], which is a candidate gene prioritization algorithm, indeed enables to underpin the list of most significantly interconnected genes, termed as hub genes or leader genes (Figures 2 and 3). This algorithm has been exploited to shed light on the molecular mechanisms of tolerance to kidney transplant, showing the gene interaction network expanded around *TMTC3/SMILE*, a gene differentially expressed in transplanted immunosuppressive-free subjects [15]. Some of these genes (*HTATIP/KAT5*, *ARRB2* and *ATF2*) have been rarely described as predictors of clinical outcome to renal graft in the extant literature, whilst the others (*c-JUN*, *TP53*, *MAPK14*, *XBP1* and *NPHS1*) were already known to be associated with kidney transplant. The panel made up of the previously computed hub genes has been validated mining the Gene Expression Omnibus (GEO) database, a publically available repository of gene microarrays. The pooled analysis of their expression has confirmed their relevance in the biological processes leading to tolerance to kidney allograft, both for the expression in blood and in kidney tissue. Gene Ontology (GO) analysis has enabled to investigate the main pathways involved in the response to kidney transplant (Figure 2). The Pearson statistical analysis has shown correlation between expression in blood and in kidney tissue (Figure 3) [16].

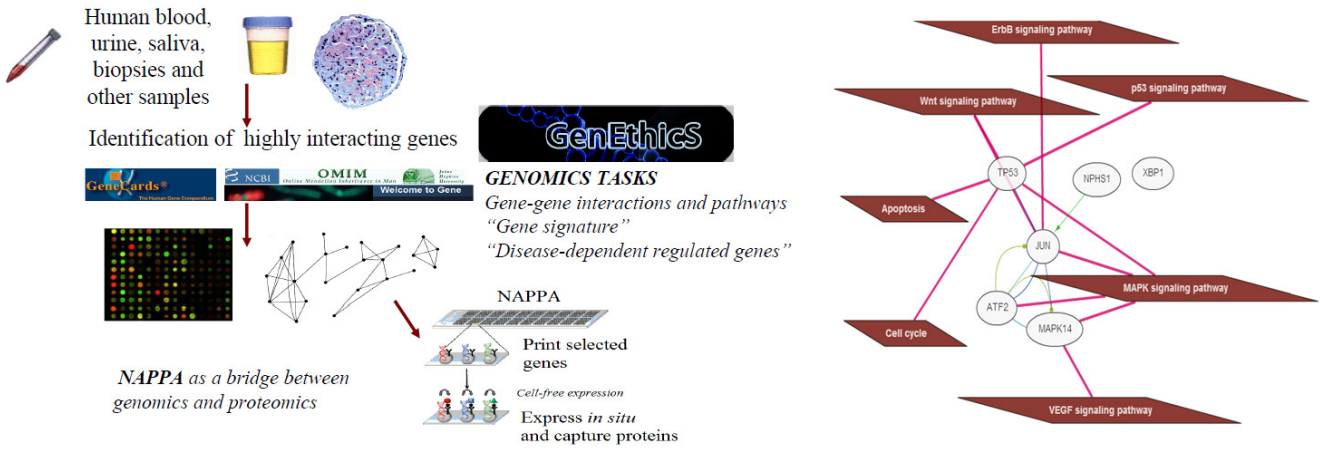

Figure 2: The genomics branch of the previously (Figure 1) introduced protocol of integrated nanoproteogenomics approach (left) and an example of application to kidney transplant (right) showing the pathways involved in the tolerance process to kidney allograft.

Genomics alone is not able to shed light on complex biological processes if not extensively coupled with proteomics. Nucleic Acid Protein Programmable Arrays (NAPPA) represents the necessary step further, being a bridge between genomics and proteomics. It enables to study proteins from the expression of selected genes (Figure 4), both with labeled technologies (Figure 4, above) and with label-free devices (Figure 4, below) [17, 18]. These selected genes can be the genes obtained with the previously mentioned candidate gene prioritization algorithm or similar approaches.

Recently, we coupled NAPPA with the Quartz Crystal Microbalance (QCM) with Dissipation factor (D factor) monitoring (QCM_D), showing that we are able to distinguish among different proteins, each one having its unique conductance curve [19]. Besides performing the genomics and proteomics task, NAPPA-based QCM_D enables to investigate and perform both pharmacogenomics and pharmacoproteomics tasks in a very effective, quick (only few minutes) and cheap way, making it particularly attractive for clinical uses.

In particular, brain tumor is one of the most aggressive forms of cancer.

Temozolomide(3-Methyl-4-oxo-3,4-dihydro-imidazo[5,1-d][1,2,3,5]tetrazine-8-carboxylic acid amide; brand name Temodar, Temodal and Temcad) is an oral antiblastic, chemically being the imidazotetrazine derivative of the alkylating/methylating agent dacarbazine and undergoing rapid chemical conversion in the systemic circulation at physiological pH to the active compound 3-methyl-(triazen-1-yl)imidazole-4-carboxamide (MTIC). Temozolomide is useful for treating brain tumors, such as the grade IV astrocytoma or glioblastoma multiforme, the relapsed grade III anaplastic astrocytoma, especially if nitrosourea- and procarbazine-refractory, as well as skin cancers like melanoma and the fungoides mycosis/Sézary syndrome. It is currently in evaluation for the treatment of other tumors, such as the relapsed primary central nervous system (CNS) lymphoma, recurrent glioma and oligodendroglioma (in the last case, replacing the classical regimen PCV, *i.e.* procarbazine-lomustine-vincristine). When it binds to the DNA, usually at

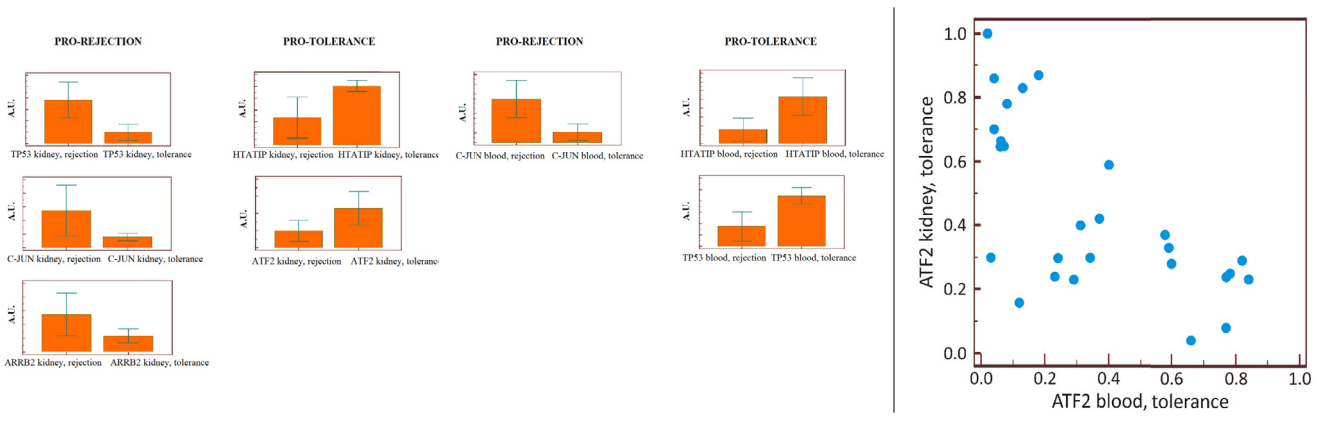

Figure 3: Differentially expressed genes (DEGs) involved in the process of tolerance to kidney allograft, as discovered exploiting Leader Gene Algorithm (LGA), validated mining the Gene Expression Omnibus (GEO) repository of gene microarrays (Left). The Pearson's correlation plot shows the statistically significant correlation between expression in blood and in kidney tissue (Right).

Of particular clinical interest is indeed the pharmacodynamics and pharmacokinetics characterization of antiblastic drugs as cancer is one of the major issues to be still addressed in the field of clinical biomedicine [20].

the N-7 or O-6 positions of guanine residues, it produces O^6-methylguanine (O6MG) and this abduct causes the activation of futile DNA mismatch repair (MMR), as well as DNA double-strand breaks (DSBs), G(2) arrest and ultimately

cell death. The activation of the molecular mechanisms of MMR is quite a complex biological process that requires different protein-protein interactions, such as the Mre11/Rad50/Nbs1 (MRN complex), the Proliferating Cellular Nuclear Antigen (PCNA) complex and the gamma-H2AX and 53BP1 foci [21]. Unfortunately, some cells can escape from this mechanism producing a protein known as O^6-alkylguanine DNA alkyltransferase (AGT), encoded by the O^6-methylguanine-DNA methyltransferase (*MGMT*) gene. Recently, scientists have been able to find and characterize some biomarkers of resistance to temozolomide, such as *MLH1*, which is also an important marker of survival rate in patients with glioblastoma [21-25].

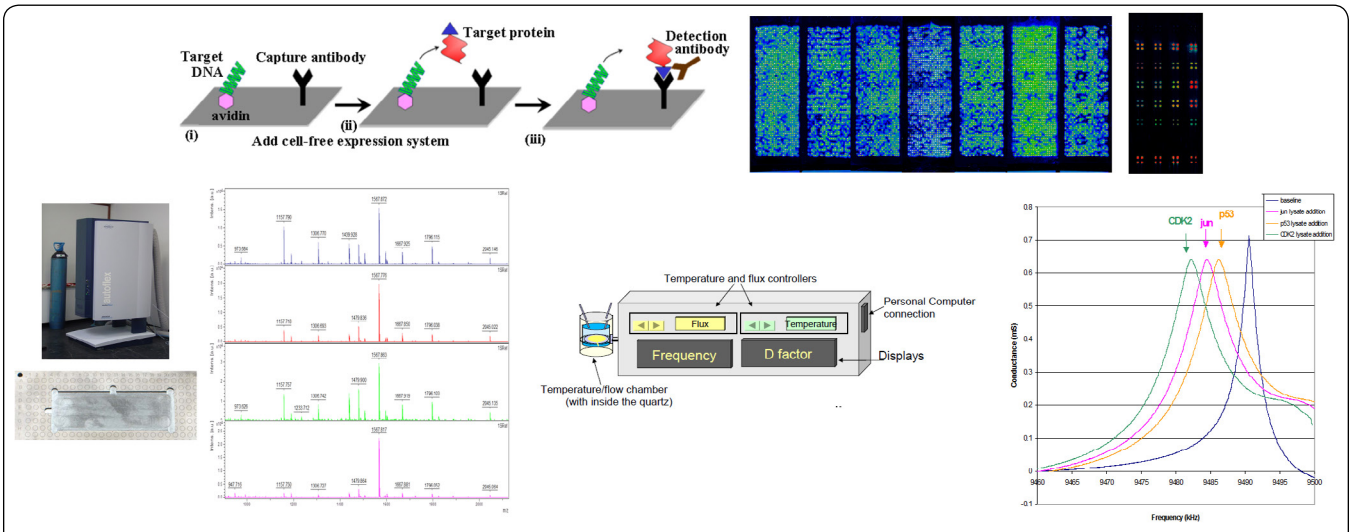

Figure 4: Schematic representation of Nucleic Acid Programmable Protein Arrays (NAPPA) technology for Mass Spectrometry (MS) with SNAP. In each spot a mixture of plasmid DNA, BSA and anti-GST antibodies is printed and immobilized on cysteamine coated surface. The antibody is responsible for the capture of the freshly expressed proteins that are tagged, at one of their ends, with a GST tail. The proteins are translated using an in vitro transcription–translation system (IVTT) (top). Fluorescence-based technologies (top, right) and label-free technologies, namely Quartz Crystal Microbalance with Dissipation Monitoring (QCM_D) coupled with NAPPA and Mass Spectrometry (MS) (bottom).

Another innovative approach we developed is given by coupling NAPPA with the SNAP tag *Escherichia coli* coupled cell-free expression system and Mass Spectrometry (MS) (in particular, the Matrix Assisted Laser Desorption Ionization Time-of-Flight (MALDI-TOF) Bruker Ultraflex) with the goal of implementing a standardized procedure of identification of biomarkers in clinical settings and to analyze the protein-protein interaction occurred on NAPPA array using label-free technology [26]. We employed the process "Protein synthesis Using Recombinant Elements" (PURE) system, which, due to its high complexity, needs *ad hoc* in-house developed bioinformatics tools to be analyzed. The PURE system represents a step towards a totally defined *in vitro* transcription/translation system (IVTT), thus avoiding the "black box" nature of the cell extract. The immediate advantage is the significantly reduced level of all contaminating activities and the *Escherichia coli* IVTT machinery in respect to the rabbit reticulocyte lysate (RRL) or human lysate, which is totally characterized and thereby represents an advantage for the subsequent MS analysis of the results. The presence of "background" molecules, in fact, represents the main obstacle to these MS data interpretation. For this latter reason "An R Script for Mass Spectrometry Data Preprocessing before Data Mining" (SpADS) was implemented [27]. SpADS provides useful pre-processing functions, such as binning, peak extractions, spectra background subtraction and dataset managing. Moreover, in its final version, it is able to perform peak recognition, as well as amplitude independent subtraction. The MS samples are obtained from SNAP-NAPPA spots printed on gold coated glass slides in higher density, in order to obtain an amount of protein appropriate and suitable for MS analysis. Spots of 300 microns were printed in 12 boxes, each box with 100 identical spots. The sample of immobilized genes used as test cases were all of clinical interest and implicated in the process of mutagenesis and carcinogenesis: namely, *p53*_human (cellular tumor antigen p53); *CDK2*_human (cyclin-dependent kinase type 2); *SRC*_human-SH2 (the SH2 domain of proto-oncogene tyrosine-protein kinase), *PTPN11* (human-SH2, the SH2 domain of tyrosine-protein phosphatase non-receptor type 11).

Materials and Methods

QCM_D nanoconductimetry

The QCM_D instrument was developed by Elbatech (Elbatech srl, Marciana – LI, Italy). The quartz was connected to a radio frequency (RF) gain-phase detector (Analog Devices, Inc., Norwood, MA, USA) and was driven by a precision direct digital synthesis (DDS; Analog Devices, Inc.) around its resonance frequency, thus acquiring a conductance *versus* frequency curve ("conductance curve") that shows a typical Gaussian behaviour. The conductance curve peak was at the actual resonance frequency, while the shape of the curve indicated how the viscoelastic effects of the surrounding layers affected the oscillation. The QCM_D software, QCMAgic-Q5.3.256 (Elbatech srl), allows to acquire the conductance curve or the frequency and dissipation factor variation *versus* time. In order to have a stable control of the temperature, experiments were conduced in a temperature chamber. Microarrays were produced on standard nanogravimetry quartz used as highly sensitive transducers. The QC expressing proteins consisted of 9.5 MHz, AT-cut quartz crystal of 14 mm blank diameter and 7.5 mm electrode

diameter, produced by ICM (Oklahoma City, OK, USA). The electrode material was 100 Å Cr and 1,000 Å Au and the quartz was embedded into glass-like structures for easy handling. The NAPPA-QC arrays were printed with 100 spots per QC. Quartz gold surfaces were coated with cysteamine to allow the immobilization of the NAPPA printing mix. Briefly, quartzes were washed three times with ethanol, dried with Argon and incubated overnight at 4°C with 2 mM cysteamine. Quartzes were then washed three times with ethanol to remove any unbound cysteamine and dried with Argon. Plasmid DNA coding for GST tagged proteins were transformed into *E. coli* and the DNA was purified using the NucleoPrepII anion exchange resin (Macherey Nagel, Inc., Bethlehem, PA, USA). The NAPPA printing mix was prepared with 1.4 μg/μl DNA, 3.75 μg/μl BSA (Sigma-Aldrich, Milan, Italy), 5 mM BS3 (Pierce, Rockford, IL, USA) and 66.5 μg polyclonal capture GST antibody (GE Healthcare Life Sciences, Piscataway Township, NJ, USA). Negative controls, named master mix (hereinafter abbreviated as "MM"), were obtained replacing DNA for water in the printing mix. Samples were incubated at room temperature for 1 hour with agitation and then printed on the cysteamine-coated gold quartz using the Qarray II from Genetix. In order to enhance the sensitivity, each quartz was printed with 100 identical features of 300 microns diameter each, spaced by 350 microns center-to-center.

The human cDNAs immobilized on the NAPPA-QC were: *CYP11A1* (cytochrome P450, Family 11, Subfamily A, Polypeptide 1), *MLH1* (mutL homolog 1) and *POLB* (a DNA polymerase). Gene expression was performed immediately before the assay following the protocol described in more details in our previous articles. Briefly, *in vitro* transcription and translation were performed using HeLa lysate mix (1-Step Human Coupled IVTT Kit; Thermo Fisher Scientific Inc.), prepared according to the manufacturers' instructions. The quartz, connected to the nanogravimeter inside the incubator, was incubated for 10 min at 30°C with 40 μl of HeLa lysate mix for protein synthesis and, then, the temperature was decreased to 15°C for a period of 5 min to facilitate protein binding on the capture antibody (anti-GST). After the protein expression and capture, the quartz was removed from the instrument and washed 3 times at room temperature in 500 mM NaCl PBS. The protocol described above was followed identically for both negative control QC (the one with only MM, *i.e*, all the NAPPA chemistry except the cDNA) and protein displaying QC. After protein expression, capture and washing, the QCs were used for the interaction studies. QC displaying the expressed protein was spotted with 40 μl of protein/drug solutions in PBS at increasing concentrations at 22°C.

We analyzed the interaction between CYP11A1 and cholesterol, both in solution and in blood, to acquire information on the binding kinetics. After protein expression and capture, CYP11A1-expressing QC was positioned in the flow chamber and exposed to a flow of a 50 μM cholesterol (Sigma-Aldrich) solution in 30% sodium cholate (Sigma-Aldrich) at 0.02 ml/min flow rate for 10 min at 22°C. We used cytochrome P450scc (CYP11A1) for the detection of cholesterol (Sigma-Aldrich) because of its specificity.

For the pharmacoproteomic experiment, we also tested the possibility to analyze drug-protein interactions in QC displaying multiple proteins. For this aim, we co-printed cDNA for *POLB* and *MLH1* on a single QC. We analyzed the interaction response to Temodar on both NAPPA-expressed QCs. We analyzed the interaction between MLH1, pol B and temozolomide drug solutions at different concentrations to analyze the binding kinetics. After protein expression and capture, the expressing QC was spotted, in sequence, with 40 μl of temozolomide solutions of 1 μg/ml, 2 μg/ml, 5 μg/ml, 10 μg/ml, 20 μg/ml, 50 μg/ml, 100 μg/ml and 200 μg/ml concentration.

MS of NAPPA SNAP

As far as the MS experiments are concerned, we analyzed by MALDI-TOF MS four copies of SNAP-NAPPA slides with 7×7 spots per box and four copies of slides with 10×10 spots per box. The results were extremely reproducible both with respect to 7×7 spots/box and 10x10 spots/box that with respect to the different spectrometers and no significant difference was appreciable. We conducted two parallel identifications, the first through the matching algorithm comparing blinded and known samples in the experimental mass lists and the second submitting experimental mass lists to databank search. We submitted the experimental mass list obtained for the known samples (p53, CDK2, Src-SH2 and PTPN11- SH2) to MASCOT data bank search. The matching of the results in human database allowed us to identify with a good score albumin (ALBU_HUMAN serum albumin) presumably due to some peptides that are common also to BSA. No other human proteins were identified. We performed a search against bacterial database; for all the samples we identified approximately the same proteins (essentially from the bacterial lysate). MALDI-TOF data analysis Data identified essentially proteins from SNAP-NAPPA chemistry and from bacterial lysate. These results were not surprising considering the background signal and the high complexity of the spectra of the analyzed samples. Moreover, one should bear in mind that the concentration of the proteins expressed and captured on the array is, at least in solution; hundred times lower than those of *E. coli* lysate components.

Results and Discussion

As already extensively explained in our previous articles [9, 11-13, 17-19], QCM_D measures were calibrated both for frequency and for *D* factor shifts. The calibration curve equations (obtained with Ordinary Least Squares methods, OLS) are:

$\Delta f = -7.16 - 231.18\ m$; with $r^2 = 0.9986$,
and $D = 0.831 + 0.286\ \eta$; with $r^2 = 0.9990$.

We analyzed the conductance curves acquired in NAPPA-QCs in different steps of the expressing and capturing process: after the addition of human IVTT lysate at 30°C ("IVTT addition"), *i.e.* prior protein expression; after 10 minutes from the addition of human IVTT lysate, *i.e.* after protein expression ("IVTT addition 10 min"); after the final washing process with PBS ("Post-wash").

Conductometric monitoring of enzyme-substrate and drug-protein interactions is of fundamental importance in the field of molecular pharmacology.

The P450scc-cholesterol interaction has been well characterized in the extant literature and the results obtained have been satisfactorily compared with those in literature [28].

From Figure 5, left, the decrease in the frequency (f) due to the human IVTT lysate addition is evident. There is also a change in the viscoelastic properties of the quartzes after the human IVTT lysate addition leading to a measurable increase of the bandwidth (Γ). During the incubation, on the contrary, the frequency and bandwidth variations were minimal. This effect could be related to two main causes: first, merely due to the IVTT lysate addition on the QC surface - when the QC comes in contact with a solution the frequency decreases depending upon the viscosity and the density of the solution and there is a decrement in damping the resonant oscillation - and the second, due to the change of the composition of both QC surface and IVTT lysate after gene expression, protein synthesis and immobilization. The conductance curves acquired after PBS washing evidenced the further changes of solution in contact with the QC.

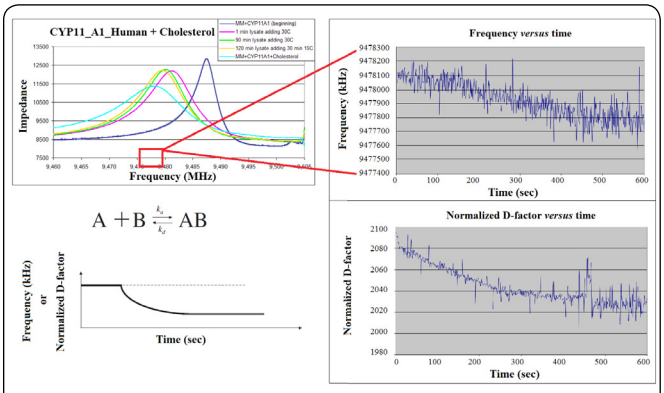

Figure 5: QCM_D conductance curves for CYP11A1-sterol interaction both in static (left) and in flow (right) conditions. Equation for mathematical modeling and data analysis is also shown (bottom, left).

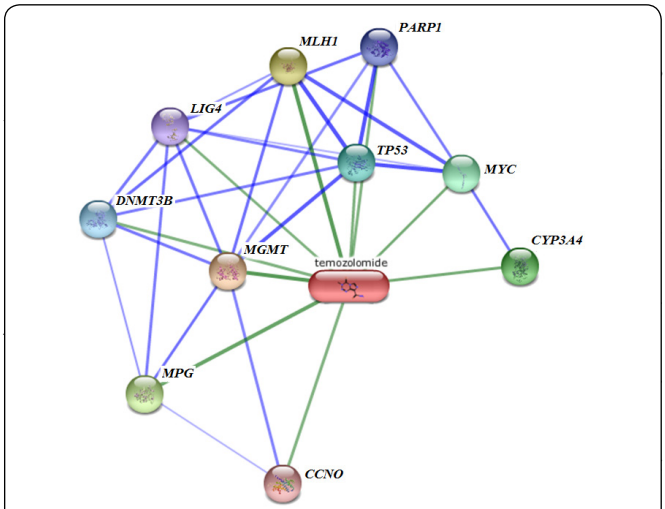

Figure 6: Bioinformatics predictions of genes interacting with temozolomide (using STITCH, http://stitch.embl.de/).

Figures 8 and 9 depict the conductance curves of reference quartz (master mix) plus temozolomide solutions at increasing concentrations (Figure 8) and the conductance curves for two NAPPA-QCs co-expressing *MLH1* and *POLB* (Figure 9, multi-gene experiment). These data pointed to a unique conductance curve shape for each protein and suggested the possibility to identify the expressed proteins by QCM-D even when combined on the same expressing QC.

Moreover, we assessed the reproducibility of the QCM_D measurements, computing the coefficient of variation (C_V, or σ^*) for each experiment using the following equation:

$\sigma^* = \sigma/\mu$,

where σ is the standard deviation and μ is the mean.

C_V values are usually very low, confirming the repeatability of the experiments and the validity and portability of the technique. In our hands, NAPPA-based QCM_D proved to have an intra-assay overall C_V of 5 % (range, 3.3 -8.0 %).

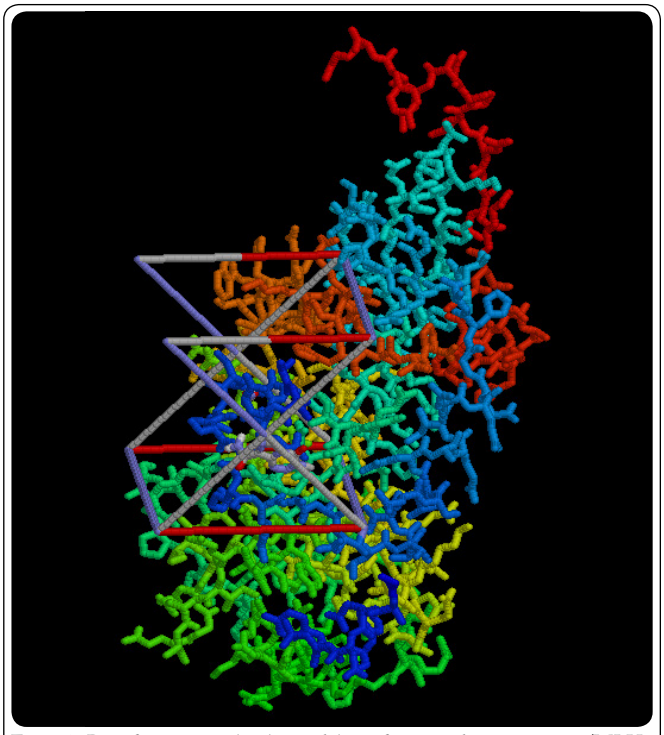

Figure 7: Bioinformatics molecular modeling of protein-drug interaction (MLH1 and temozolomide).

The MS coupled with *ad hoc*-implemented bioinformatics, as it was expected due to the high complexity of the NAPPA-SNAP system, gave quite encouraging results improving earlier findings with MS without SNAP that were very complex and, thus, a bioinformatics tool had to be developed *ad hoc* for their analysis. The MS samples were realized by printing SNAP-NAPPA spots on gold coated glass slides in a special geometry in order to obtain an amount of protein appropriate for MS analysis. The samples were printed in 12 boxes of 7×7 spots per box. One box apiece was reserved to the sample genes (*p53*, CDK2, *SH2-Src* and *SH2-PTPN11*), two boxes were negative controls (MM) and reference samples, while six boxes were printed with the sample genes in an order blinded to the researcher who performed the MS analysis. We conducted two parallel identifications, the first through the matching algorithm comparing blinded and known samples in the experimental mass lists and the second submitting experimental mass lists to databank search. The databank search of samples in the experimental mass lists obtained by MALDI-TOF or LC-ESI-MS provided the identification, with significant scores, of molecules of MM or *E. coli* lysate (Figure 4). Different strategies have been addressed to overcome the presence of these "background" molecules that represented

the main obstacle to the sample identification. Experimental master mix plus *E. coli* lysate mass lists have been subtracted to samples of the experimental mass lists and the results have been submitted to MASCOT databank search. Unfortunately, this strategy did not give statistically significant results on MS of these SNAP NAPPA arrays, with the best identification being 22% for the CDK2 sample and poor clustering even on known proteins, apparently worse if compared with those relative to the old MS NAPPA version, presented by Spera et al. [29]. By pursuing the coupling of our newly developed software SpADS to K Means Cluster algorithm we obtained good results both for known and unknown protein identification, up to 67% correct score, quite better than earlier MS without SNAP. A conservative rule of thumb suggests that using at least hundred times more MS spectra it is possible to identify the unknown protein (a minimum of hundred rather than 1 as was in the limiting worst case and rather than 8 as was in the best case). The results obtained to this point are, thereby, encouraging even with a quite low number of MS spectra so far acquired and without the subtraction of *ab initio* known MS spectra of *E. coli* lysate. As we have recently shown in more detail [30], the performed subtraction of the theoretical values of some lysate recombinant *E. coli* components, at least partially, from the experimental MS spectra, gave promising results (Figure 10).

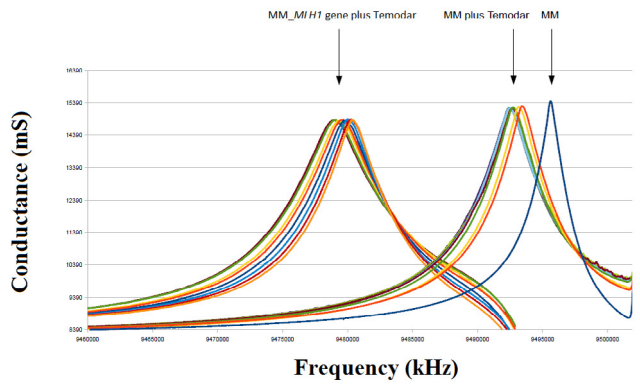

Figure 8: QCM_D conductance curves for MM_MLH1 interacting with temozolomide at increasing concentrations.

Conclusions

We developed a coherent approach by integrating genomics and proteomics that could overcome the drawbacks and pitfalls of the traditional laborious and time-consuming labeled and fluorescence-based experimental procedures.

This, taken together with the unique properties of proteins obtained with Langmuir-Blodgett (LB)-based crystallography [31-38] that can enable new strategies for drug design (work in progress), makes the goal of cancer control tremendously ambitious.

QCM_D enables scientists and physicians to test chemical-proteins in a quick and effective way. Summarizing all the experiments we have so far carried out, QCM_D is able to discriminate among dozens of molecules and chemicals, each one having its unique conductance curve shape. Being label-free, QCM_D is extremely powerful and promising in cancer control. We presented the results obtained applying our innovative conductometer realized by combining NAPPA technology with QCM_D, for the characterization of protein-protein, protein-sterol and protein-drug interactions in a multiparametric way taking advantage of the multiple information provided by the analysis of the conductance curves (*i.e.* conductance, viscoelasticity and adsorbed mass).

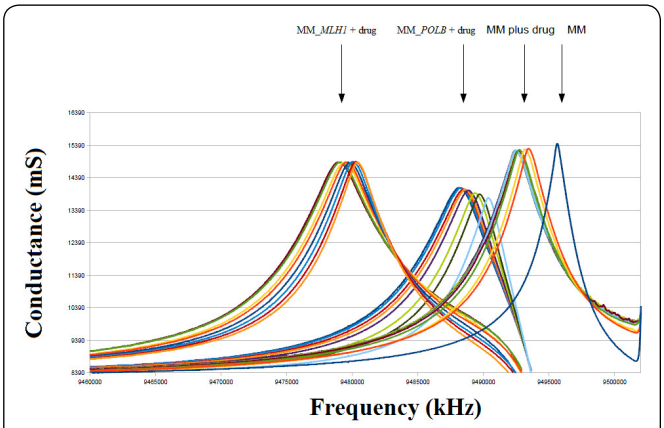

Figure 9: QCM_D conductance curves for MM_MLH1 and POLB interacting with temozolomide at increasing concentrations.

Moreover, through our conductometer, we acquired information on the kinetic constant of enzymatic interaction. Results about the sensitivity and selectivity of the original prototype have been extensively presented in previous papers that we have here reviewed. The data presented in this overview have been obtained employing a further improved version, both flow and static, of our conductometer. An interesting implication for potential clinical applications concerned the possibility to drastically reduce the time of protein expression and capture under our experimental conditions. We noticed that 15 minutes after IVTT lysate addition peak frequency and bandwidth of the curves did not change, likewise after few minutes at 15°C, for protein capture. We deduced from these results that the protein expression took place in the first minutes and that also their capture needed only few minutes. The results presented seem to confirm our hypothesis. The conductance curves obtained showed that protein expression and capture, as well as protein-protein interactions were successfully performed. The QCM_D instrument we used allowed us to monitor in real-time the trend of *D* factor and *f* during the interaction between different molecules of high clinical interest, especially for oncologists, both in solution and in blood. We, thus, demonstrated the versatility of the NAPPA-QC biosensors for the detection of protein-protein interactions, protein-sterol and protein-drug interaction. Due to the simplicity with which new NAPPA-QC biosensors can be generated and to the successful application on clinical research [39], we envision the use of this platform for the development of biosensors for other applications, including, but not limited to, protein-small molecules, protein-lipids and protein-DNA.

Also, the ongoing research in the field of MS coupled with NAPPA and SNAP is giving, as shown recently [26, 30], encouraging results in the study of protein-protein interaction, a topic relevant for cancer control. We strongly believe that these efforts can be precious in the field of personalized oncology.

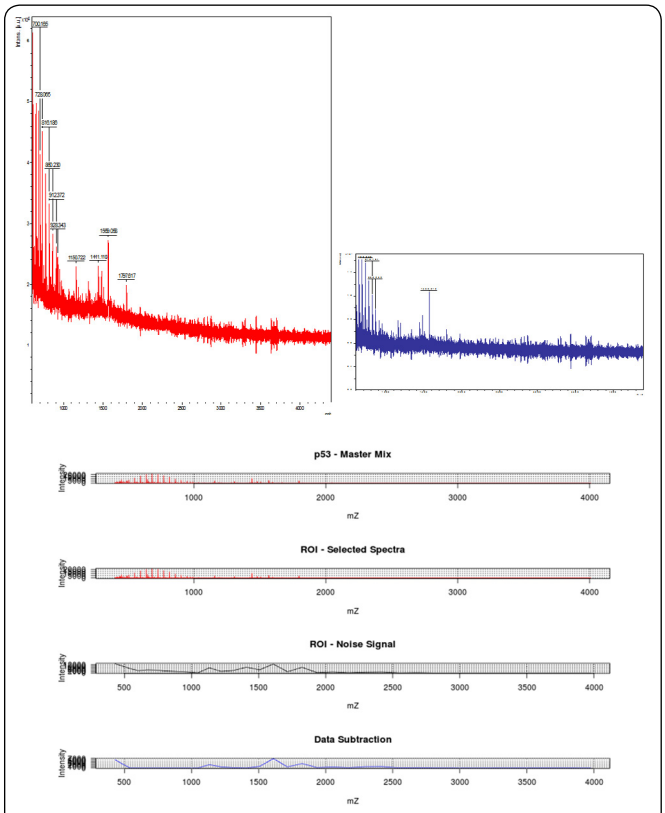

Figure 10: MS-SNAP spectra (left) and MM spectra (as background, right) properly aligned.

Funding Sources

This work was supported by FIRB Nanobiosensors (ITALNANONET RBPR05JH2P_003) of MIUR (Ministero dell'Istruzione, Università e Ricerca) to Claudio Nicolini University of Genoa and by a grant Funzionamento by MIUR (Ministero dell'Istruzione, Università e Ricerca) to Fondazione El.B.A.Nicolini.

References

1. Yan Q. 2014. Pharmacogenomics in drug discovery and development. Preface. *Methods Mol Biol* 1175: v-vii.
2. Chang WC. 2014. Pharmacogenomics in personalized medicine and drug metabolism. *Biomed Res Int*: 897963. doi: 10.1155/2014/897963
3. Hess S. 2013. The emerging field of chemo- and pharmacoproteomics. *Proteomics Clin Appl* 7(1-2): 171-180. doi: 10.1002/prca.201200091
4. Yu LR. 2011. Pharmacoproteomics and toxicoproteomics: the field of dreams. *J Proteomics* 74(12): 2549-2553. doi: 10.1016/j.jprot.2011.10.001
5. Vaiopoulou A, Gazouli M, Karikas GA. 2013. Pharmacogenomics: current applications and future prospects towards personalized therapeutics. *J BUON* 18(3): 570-578.
6. Jain KK. 2004. Role of pharmacoproteomics in the development of personalized medicine. *Pharmacogenomics* 5(3): 331-336. doi:10.1517/phgs.5.3.331.29830
7. Nicolini C. 2006. Nanogenomics for medicine. *Nanomedicine (Lond)* 1(2): 147-152. doi:10.2217/17435889.1.2.147
8. Nicolini C. 2010. Nanogenomics in medicine. *Wiley Interdiscip Rev Nanomed Nanobiotechnol* 2(1): 59-76. doi:10.2217/17435889.1.2.147
9. Bragazzi NL, Spera R, Pechkova E, Nicolini C. 2014. NAPPA-based nanobiosensors for the detection of proteins and of protein-protein interactions relevant to cancer. *J Carcinog Mutagen* 5(3):166 doi: 10.4172/2157-2518.1000166
10. Pechkova E, Bragazzi NL, Nicolini C. 2014. Advances in nanocrystallography as a proteomic tool. *Adv Protein Chem Struct Biol* 95: 163-191. doi: 10.1016/B978-0-12-800453-1.00005-1
11. Bragazzi NL, Pechkova E, Nicolini C. 2014. Proteomics and proteogenomics approaches for oral diseases. *Adv Protein Chem Struct Biol* 95: 125-162. doi: 10.1016/B978-0-12-800453-1.00004-X
12. Nicolini C, Bragazzi N, Pechkova E. 2012. Nanoproteomics enabling personalized nanomedicine. *Adv Drug Deliv Rev* 64(13): 1522-1531. doi: 10.1016/j.addr.2012.06.015
13. Nicolini C, Pechkova E. 2010. An overview of nanotechnology-based functional proteomics for cancer and cell cycle progression. *Anticancer Res* 30(6): 2073-2080.
14. Bragazzi NL, Nicolini C. 2013. A leader genes approach-based tool for molecular genomics: from gene-ranking to gene-network systems biology and biotargets predictions. *J Comput Sci Syst Biol* 6: 165-176. doi: 10.4172/ jcsb.1000113
15. Racapé M, Bragazzi N, Sivozhelezov V, Danger R, Pechkova E, et al. 2012. SMILE silencing and PMA activation gene networks in HeLa cells: comparison with kidney transplantation gene networks. *J Cell Biochem* 113(6): 1820-1832. doi: 10.1002/jcb.24013
16. Bragazzi NL, Nicolini C. 2014. Nanogenomics for personalized nanomedicine: an application to kidney transplantation. *Cell Mol Biol* 60: 115. doi: 10.4172/1165-158X.1000115
17. Nicolini C, Adami M, Sartore M, Bragazzi NL, Bavastrello V, et al. 2012. Prototypes of newly conceived inorganic and biological sensors for health and environmental applications. *Sensors (Basel)* 12(12): 17112-17127. doi: 10.3390/s121217112
18. Nicolini C, Bragazzi N, Pechkova E. 2013. From nanobiotechnology to organic and biological monitoring of health and environment for biosafety. *Biosafety* 2(3): 116. doi: 10.4172/2167-0331.1000116
19. Spera R, Festa F, Bragazzi NL, Pechkova E, LaBaer J, et al. 2013. Conductometric monitoring of protein-protein interactions. *J Proteome Res* 12(12): 5535-5547. doi: 10.1021/pr400445v
20. Wulfkuhle JD, Edmiston KH, Liotta LA, Petricoin EF 3rd. 2006. Technology insight: pharmacoproteomics for cancer--promises of patient-tailored medicine using protein microarrays. *Nat Clin Pract Oncol* 3(5): 256-268. doi:10.1038/ncponc0485
21. Mirzoeva OK, Kawaguchi T, Pieper RO. 2006. The Mre11/Rad50/Nbs1 complex interacts with the mismatch repair system and contributes to temozolomide-induced G2 arrest and cytotoxicity. *Mol Cancer Ther* 5(11): 2757-2766. doi: 10.1158/1535-7163.MCT-06-0183
22. Querfeld C, Rosen ST, Guitart J, Rademaker A, Pezen DS, et al. 2011. Multicenter phase II trial of temozolomide in mycosis fungoides/sezary syndrome: correlation with O6-methylguanine-DNA methyltransferase and mismatch repair proteins. *Clin Cancer Res* 17(17): 5748-5754. doi: 10.1158/1078-0432.CCR-11-0556
23. Shinsato Y, Furukawa T, Yunoue S, Yonezawa H, Minami K, et al. 2013. Reduction of MLH1 and PMS2 confers temozolomide resistance and is associated with recurrence of glioblastoma. *Oncotarget* 4(12): 2261-2270.
24. Stark AM, Doukas A, Hugo HH, Mehdorn HM. 2010. The expression of mismatch repair proteins MLH1, MSH2 and MSH6 correlates with the Ki67 proliferation index and survival in patients with recurrent glioblastoma. *Neurol Res* 32(8): 816-820. doi: 10.1179/016164110X12645013515052
25. von Bueren AO, Bacolod MD, Hagel C, Heinimann K, Fedier A, et al. 2012. Mismatch repair deficiency: a temozolomide resistance factor in medulloblastoma cell lines that is uncommon in primary medulloblastoma tumours. *Br J Cancer* 107(8): 1399-1408. doi: 10.1038/bjc.2012.403
26. Nicolini C, Spera R, Festa F, Belmonte L, Chong S, et al. 2013. Mass spectrometry and florescence analysis of Snap-Nappa arrays expressed using E. coli cell_free expression system. *J Nanomed Nanotechnol* 4(5): 181. doi: 10.4172/2157-7439.1000181

27. Belmonte L, Spera R, Nicolini C. 2013. SpADS: An R script for mass spectrometry data preprocessing before data mining. *J Comput Sci Syst Biol* 6(5): 298-304. doi: 10.4172/jcsb.1000125

28. Ghisellini P, Paternolli C, Antonini M, Nicolini C. 2004. P450scc mutant nanostructuring for optimal assembly. *IEEE Trans Nanobioscience* 3(2): 121-128. doi: 10.1109/TNB.2004.828267

29. Spera R, Labaer J, Nicolini C. 2011. MALDI-TOF characterization of NAPPA-generated proteins. *J Mass Spectrom* 46(9): 960-965. doi: 10.1002/jms.1976

30. Nicolini C, Belmonte L, Spera R, Pechkova E. 2015. Spads and SNAP-NAPPA microarrays for biomarkers identification in humans: background subtraction in mass spectrometry with E. coli cell-free expression system. *J Mol Biomark Diagn* 6(1): 214. doi: 10.4172/2155-9929.1000214

31. Bozdaganyan M, Bragazzi NL, Pechkova E, Shaitan KV, Nicolini C. 2014. Identification of best protein crystallization methods by molecular dynamics (MD). *Crit Rev Eukaryot Gene Expr* 24(4): 311-324. 10.1615/CritRevEukaryotGeneExpr.2014010201

32. Bragazzi NL, Pechkova E, Scudieri D, Terencio TB, Adami M, et al. 2012. Recombinant laccase: II. Medical biosensor. *Crit Rev Eukaryot Gene Expr* 22(3): 197-203. 10.1615/CritRevEukarGeneExpr.v22.i3.30

33. Gebhardt R, Pechkova E, Riekel C, Nicolini C. 2010. In situ muGISAXS: II. Thaumatin crystal growth kinetic. *Biophys J* 99(4): 1262-1267. doi: 10.1016/j.bpj.2010.03.068

34. Pechkova E, Belmonte L, Riekel C, Popov D, Koenig C, Nicolini C. 2013. Laser-microdissection of protein crystals down to submicron dimensions. *J Nanomed Nanotechol* S15: 002. doi: 10.4172/2157-7439.S15-002

35. Pechkova E, Bragazzi N, Bozdaganyan M, Belmonte L, Nicolini C. 2014. A review of the strategies for obtaining high-quality crystals utilizing nanotechnologies and microgravity. *Crit Rev Eukaryot Gene Expr* 24(4): 325-339. doi: 10.1615/CritRevEukaryotGeneExpr.2014008275

36. Gebhardt R, Pechkova E, Riekel C, Nicolini C. 2010. In situ muGISAXS: I. Experimental setup for submicron study of protein nucleation and growth. *Biophys J* 99(4): 1256-1261. doi: 10.1016/j.bpj.2010.03.069

37. Pechkova E, Scudieri D, Belmonte L, Nicolini C. 2012. Oxygen-bound Hell's gate globin I by classical versus LB nanotemplate method. *J Cell Biochem* 113(7): 2543-2548. doi: 10.1002/jcb.24131

38. Pechkova E, Sivozhelezov V, Belmonte L, Nicolini C. 2012. Unique water distribution of Langmuir-Blodgett versus classical crystals. *J Struct Biol* 180(1): 57-64. doi: 10.1016/j.jsb.2012.05.021

39. Nicolini C, Spera R, Bragazzi NL, Pechkova E. 2014. Drug-protein interactions for clinical research by NAPPA QCM_D nanoconductometric assay. *Am J Biochem Biotechnol* 10(3):189-201. doi: 10.3844/ajbbsp.2014.189.201